REINFORCING FOLDING BOARD BOXES BY PRINTING A PLA PATTERNED GRID ON THEIR PANELS: A NEW APPROCAH FOR LIGHTWEIGHTING STIFF PACKAGING

Nicolas Bonnet, Jérémie Viguié, Davide Beneventi, Didier Chaussy

REINFORCING FOLDING BOARD BOXES BY PRINTING A PLA PATTERNED GRID ON THEIR PANELS: A NEW APPROCAH FOR LIGHTWEIGHTING STIFF PACKAGING

Nicolas Bonnet, Jérémie Viguié*, Davide Beneventi, Didier Chaussy

Univ. Grenoble Alpes, CNRS, Grenoble INP[a], LGP2, 38000 Grenoble, France

[a]Institute of engineering Univ. Grenoble Alpes* Corresponding author

e-mail: jeremie.viguie@lgp2.grenoble-inp.fr

ABSTRACT

The potential of printing stiffeners of polylactic acid (PLA) by Fused Deposition Modeling (FDM) on the panels of folding board boxes was investigated in view of reducing the board weight while maintaining the box resistance to vertical compression. Cyclic loading and unloading compression tests were performed under standard (50% RH) and humid (85% RH) environmental conditions on boxes printed with different grid patterns. By only adding 7% in weight of PLA to the whole packaging, the performance was improved by 29% under standard conditions and 60% under humid conditions when the inner surface of box panels was printed with an orthogonal-type grid. A comparison with a higher basis weight folding board suggested that 30% of raw materials could be saved. Results suggested that the grid mainly improved the elastic properties of the panels and could delay the buckling of panels and thus the box collapse. Furthermore, the grid pattern could affect the buckling shape that the panels took.

1. INTRODUCTION

Papers and boards are mostly bio-sourced, recyclable, and biodegradable materials. Regarding environmental issues, they offer an interesting alternative to plastic. Many industrial groups and major distributors are making efforts to reduce their use of plastic packaging. In

this context, the use of paperboard as lightweight stiff packaging material is growing in the food, cosmetic and drug industries. Innovative surface treatments have been developed to give paperboard the required barrier properties while guaranteeing it remains biodegradable and recyclable (Tyagi *et al.*, 2021). However, the production cost of these new packaging solutions must be reduced to make the switch from plastic to paperboard economically viable. One efficient way may be to decrease the weight of the whole packaging (*i.e.* folding board box) while maintaining a suitable level of mechanical performance (Hubbe, 2014).

Paperboard is a thick stratified paper-based material with a basis weight between 180 and 450 g/m². Each layer may be made of a specific grade of pulp. For example, in folding boxboard, the inner layers are composed of low-density mechanical pulps (lignin-rich) to provide high stiffness to the folding board structure, while chemical pulps (lignin-free) are used for the outer layers to provide strength and whiteness. Cohesion of the stratified structure is often promoted by the addition of starch-based solutions between the layers. Layers are known to have complex elastic-plastic properties (Li *et al.*, 2016). They are anisotropic (orthotropic) because of the fibre orientation and the internal stresses induced during papermaking. Usually, the main in-plane anisotropy axes are referred to as the machine direction (MD) and the cross direction (CD). Layers show also viscoelastic behaviour due to the polymeric nature of its constituents. Furthermore, damage may occur during loading (Viguié *et al.*, 2010).

Often stored and transported in stacks, folding board boxes have to withstand static and dynamic compression loads and sometimes shocks on their lateral panels. These loading conditions lead to local buckling phenomena of box panels, which result in collapsing and crushing of boxes (Viguié *et al.*, 2010; Viguié *et al.*, 2011). The occurrence of panels buckling and box collapse is also highly affected by environmental conditions (*i.e.* air humidity) (Lamb and Rouillard, 2017). As the compression resistance of the folding board box is related to the buckling behaviour of panels, it greatly depends on the bending stiffness of the folding board (Urbanik and Frank, 2006; Viguié *et al.*, 2013; Frank, 2014).

Designing ribbed plate or shell structures is relevant to improve the moment of inertia of the cross section and accordingly the bending stiffness to weight ratio of materials (Huybrechts *et al.* 1999). Indeed, these structures are widely present in nature and used extensively in transports and constructions (Wang *et al.* 2019). Bending and buckling performances are mainly controlled by the geometry of the ribs and the network they form (Akl *et al.* 2008; Wang *et al.* 2019). The mechanical performance can be specifically improved by using auxetic patterned structures (Kabir et al. 2020, Viguié *et al.*, 2021).

In this work, we investigated the potential of printing ribs of polylactic acid (PLA), by using the Fused Deposition Modeling (FDM) process, at the surface of panels of folding board boxes to improve their compression strength under standard or humid environmental conditions. PLA is a bio-based polymer, recyclable and biodegradable (under specific conditions), with good mechanical properties and an excellent ability to be processed by FDM (Valerga *et al.*, 2018). In the following, the first section is dedicated to the description of the printing approach. Then, the structural features of the printed folding board boxes are described. Their compression behaviour is displayed under different environmental conditions. Finally, results are discussed in order to give some insights on the box weight reduction that could be achieved.

2. MATERIAL & METHODS

2.1. Folding boxboard

A commercial folding board of 195 g/m² ± 4% (thickness 275 µm ± 5%) was selected. It is a stratified structure composed of one inner layer made of a mixture of chemo-thermo-mechanical pulp and sulphate pulp (chemical pulp), surrounded on each side by a layer of sulphate pulp.

2.2. Box manufacturing

The box blanks were drawn using the software ArtiosCad 5.2 (Esko, Gent, Belgium). They were cut and creased using a Kongsberg XL22 (Esko, Gent, Belgium) cutting table. The box

blank included panels, flaps, scores and a manufacturer's joint. Box dimensions were 71 x 71 x 71 mm^3 (see Fig. 1a). The crease depth used was 200 µm. Once the box was erected and glued, the inner and outer flaps covered completely the top and bottom box surfaces. Note that the cross direction (CD) of the folding board was aligned along the compression axis.

2.3. Grid printing on box panels

A 3D printed Artillery Sidewinder X1 (Artillery 3D Technology CO., Shenzhen, China) with a nozzle of diameter 600 µm was used. The PLA filament of diameter 1.75 mm was supplied by Dailyfil (Amsterdam, Netherlands). In order to enhance PLA adhesion on the folding board and to avoid delamination, PLA was printed using nozzle and bed temperatures of 220 and 70°C, respectively. Four grid patterns were printed on the flat folding board before cutting and creasing: an orthogonal (Fig. 1a), an orthogonal orientated at 45° (Fig. 1b), a sinusoidal (Fig. 1c) and a honeycomb type (Fig. 1d). The sinusoidal pattern is known to form structures with an auxetic behaviour (Ren et al. 2018). The covering ratio (i.e. % printed surface) was around 20% for each pattern, except for the sinusoidal pattern where it was slightly higher. Finally, the folding board weight was improved by 10-12% (see Table 1) and the whole box weight by 7-9% (see Table 2). Some boards were printed on the outer surface of the panels (Fig. 1a-d) and some other on the inner surface of the panels (see an example Fig. 1e). The corresponding boxes are designated as printed outside and printed inside. The width and the thickness of the printed lines were accurately measured using an Infinite Focus (Bruker Alicona, Graz, Austria). The thickness was quite regular and around 100 µm (see Fig. 1f-g).

2.4. Characterization

The bending behaviour of both printed and pristine folding boards was preliminary characterized by performing two points bending tests following ISO 2493-1. All the tests were carried out in a conditioned atmosphere at 23°C and 50% RH. Results are presented in Table 1.

Table 1. Basis weight and bending stiffness of the reference and the printed folding boards CD means cross direction, MD means ????.

		Reference	+ PLA Grid		
			Orthogonal	Honeycomb	Sinusoidal
Basis weight (g/m²)		194 ±2	216 ±2	215 ±2	218 ±2
Bending stiffness (mN.m)	MD	10.5 ±0.4	12.7 ±1.3	12.3 ±1.8	13.8 ±2.8
	CD	3.9 ±0.1	4.9 ±0.4	4.5 ±0.4	5.1 ±0.3

Box compression tests were performed using an IDM Press (IDM, San Sebastian, Spain) SC-500 (maximum axial force 5 kN, maximum crosshead velocity 500 mm/min). During the experiments, the load *F* and the axial platen displacement δ (<0) were recorded. Then, the macroscopic box axial stress was calculated as

$$\Sigma = \frac{F}{S_0} \quad (1)$$

where S_0 is defined arbitrarily as the area of the box cross section, as well as the macroscopic box axial strain

$$\varepsilon = \ln\frac{a+\delta}{a} \quad (2),$$

where *a* is the box height. Cyclic loading and unloading compression tests were performed at a constant compression velocity $\dot{\delta} = 13\ mm/min$. Four replicate experiments were carried out for each configuration. Tests were performed at 23°C in two different relative humidity conditions: 50% RH and 85% RH. Boxes were conditioned 24 hours in each atmosphere before testing. The typical evolution curve of the reference box (*i.e.* unprintred) is presented in Fig. 2a. For conditioning the boxes in humid atmosphere, a climatic chamber HPP110 (Memmert, Schwabach, Germany) was used. Then, each box was put into a transparent hermetic plastic bag and tested in the bag (see Fig. 4).

Figure 1. Pictures of boxes with panels printed on the outer surface with PLA-grid by FDM with the different patterns and their dimensions: (a) orthogonal, (b) orthogonal orientated at 45°, (c) sinusoidal and (d) honeycomb. (e) Picture of an opened box with panels printed on the inner surface. (f) Picture from the topographic measurement of the printed line of the sinusoidal pattern. (g) Evolution of the height of the printed line along its width (line represented in f).

3. RESULTS

3.1. Mechanical performance of the printed boxes

Typical loading-unloading curves of the printed boxes are shown in Figure 2. Regardless of the grid pattern and the printed side of the panels, curves could be split into the same typical stages displayed by the curve of the reference box (see Fig. 2a). Until point t1, the box axial stress $\sum$ showed a slow increase with respect to the box axial strain ε. This stage was related to the unevenness of the flaps that were levelled out as the platens began to compress the box. As the geometrical unevenness of the flaps was removed, $\sum$ increased sharply with the applied ε (as depicted between point t1 and point t2. At t2), a transition for the slope of the curve was observed. The curve still continued increasing with a lower slope until reaching a plateau. Box pictures shown in Figure 2 depict typical changes in the box shape occurring during the test. After point t2, the first visible local buckling phenomenon of the box panels appeared. Then, localized deformations occurred: creases were initiated from the corners of the box. Then the panels' buckling developed and the creases grew until joining each other. All panels buckled outwards by forming one half-wave (*i.e.* buckling mode = 1), except the box panels printed with the sinusoidal grid that buckled by forming two half-waves (*i.e.* buckling mode = 2) (Fig. 2d). In order to compare the mechanical performance of boxes, the evolution of $\sum$ at the end of each loading step (pointed as red stars in Fig. 2a) was plotted as a function of the corresponding ε, in Figure 3a when the grid was printed outside and in Figure 3b when the grid was printed inside. The slope (between t1 and t2) was the highest for the orthogonal grid and the lowest for the sinusoidal grid. The level of the plateau significantly differed following the grid pattern. The corresponding maximum $\sum$ values (noted Max$\sum$) are presented in Table 2. The highest value was reached for the orthogonal grid whatever the printed side. Moreover Max$\sum$ was systematically and significantly higher when the grid was printed inside. Indeed, the improvement (compared to the reference box) was 19% and 29%, respectively. Max$\sum$ was only slightly lower when the orthogonal grid was orientated at 45°. In contrast, the box with the sinusoidal grid had similar Max$\sum$ than the reference box when it was printed

outside and only slightly higher when it was printed inside. This behaviour could be related with the particular buckling behaviour of these panels. In the post-buckling regime, the two half-waves configuration could result in a different local stress state in the panels that could induce an early collapse of the box. The box with the honeycomb grid had an intermediate performance (between the reference box and the box printed with the orthogonal grid).

Table 2. Weight and maximum compression strength of the boxes made with the different grid patterns printed outside (Out) or inside (Int) the box, and tested under standard or humid conditions. Data for the reference (unprinted) box and a box made with a folding board of 300 g/m² basis weight were added for comparison.

		Reference	+ PLA Grid								Board
		195 g/m²		Orthogonal	*Gain*	Orthogonal 45°	*Gain*	Honeycomb	*Gain*	Sinusoidal	*Gain*	300 g/m²
Box weight (g)		8.2 ±0.1		8.8 ±0.2	*+7%*	8.8 ±0.2	*+7%*	8.8 ±0.2	*+7%*	9.0 ±0.2	*+9%*	*12.2 ±0.2*
Compression strength - Max ∑ (MPa)	50% RH	1.13 ±0.05	*Out*	1.35 ±0.06	*+19%*	1.31 ±0.08	*+16%*	1.22 ±0.11	*+8%*	1.11 ±0.04	*-2%*	*1.68 ±0.05*
			In	1.46 ±0.08	*+29%*	1.37 ±0.04	*+21%*	1.30 ±0.07	*+15%*	1.28 ±0.12	*+13%*	
	85% RH	0.52 ±0.04	*Out*	0.69 ±0.05	*+33%*	0.66 ±0.05	*+27%*	0.66 ±0.05	*+27%*	0.57 ±0.11	*+10%*	*0.77 ±0.04*
			In	0.83 ±0.04	*+60%*	0.84 ±0.04	*+61%*	0.79 ±0.03	*+52%*	0.72 ±0.04	*+38%*	

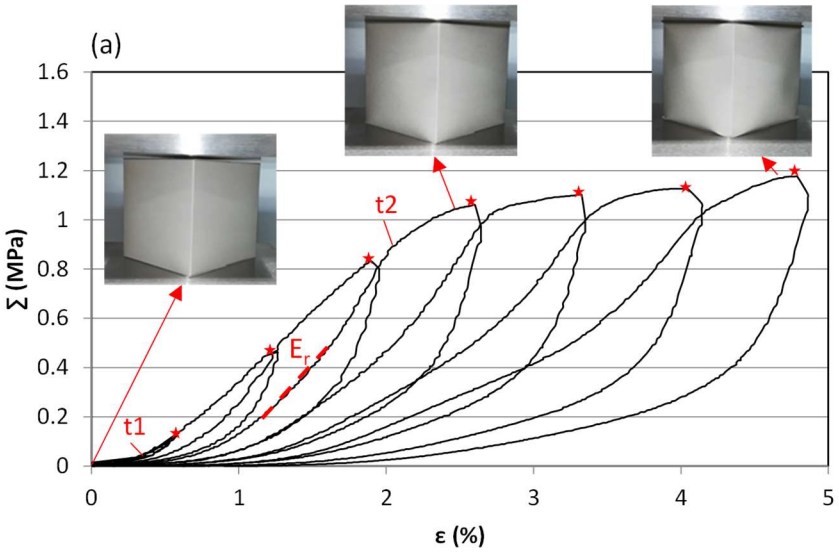
(a)
1.6
1.4
1.2
1
0.8
0.6
0.4
0.2
0
∑ (MPa)
t1
t2
E_r
0
1
2
3
4
5
ε (%)

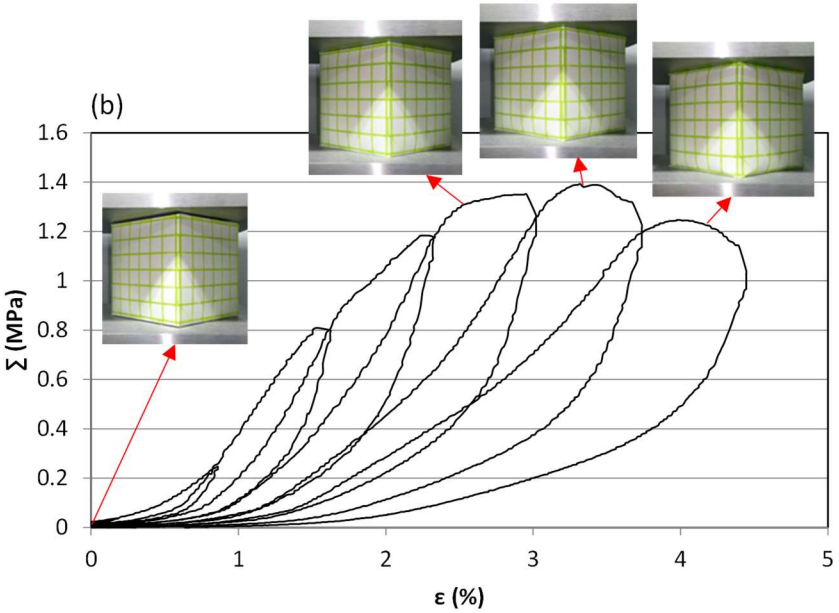
(b)
1.6
1.4
1.2
1
0.8
0.6
0.4
0.2
0
∑ (MPa)
0
1
2
3
4
5
ε (%)

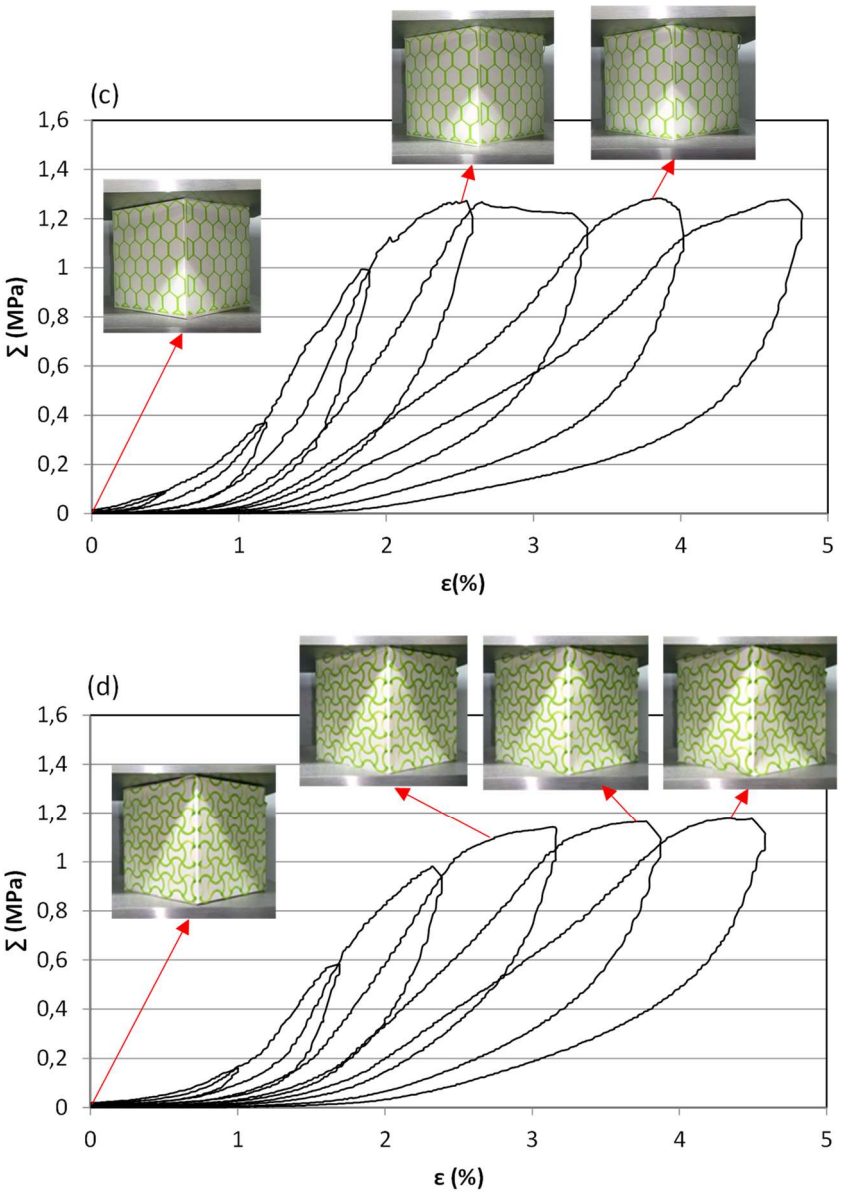

Figure 2. Loading and unloading evolution curves of (a) the reference (unprinted) box and of the boxes printed on the outer surface of the panels with the (b) orthogonal, (c) honeycomb or (d) sinusoidal grid, with pictures of the boxes at different stages of compression.

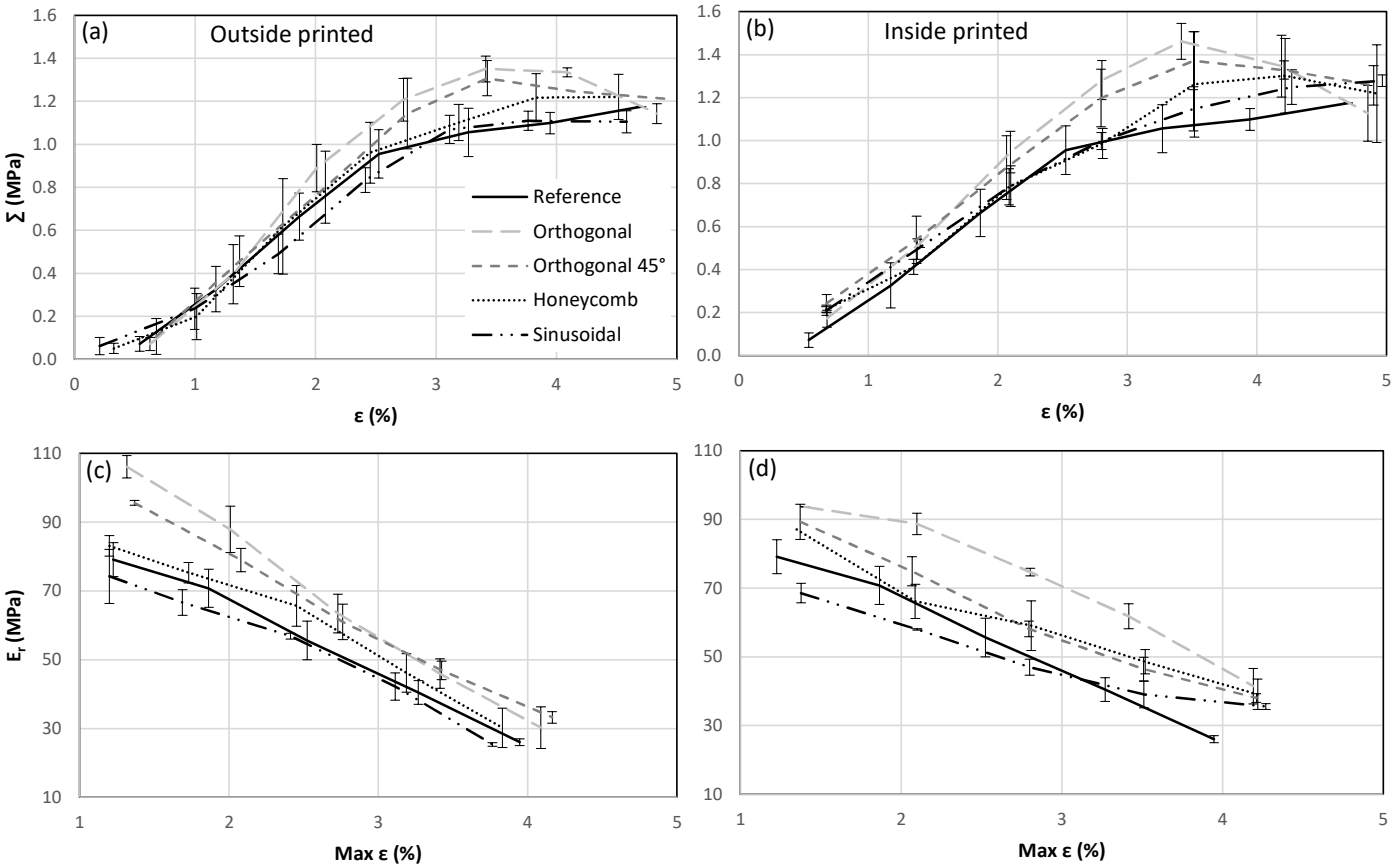

Figure 3. Evolution of the macroscopic box axial stress ∑ at the end of each loading step (red stars Fig. 2a) with the box axial strain ε for the reference box and the boxes printed with the different grid patterns on (a) the outer surface of the panels or (b) the inner surface of the panels. Evolution of the tangent modulus measured on each reloading curve E_r (see Fig. 2a) with the reached maximum strain Max ε for the reference box and the boxes printed with the different grid patterns on (c) the outer surface of the panels or (d) the inner surface of the panels.

In order to go deeper in the understanding of the contribution of the printed grid, the tangent modulus E_r was measured on each (re-)loading curve between ε = 0.2% and 0.5% (see Fig. 2a). The evolution of E_r with ε at the end of each loading step (pointed as red stars in Fig. 2a and noted Max (ε)) was plotted in Figure 3c when the grid was printed outside and in Figure 3d when the grid was printed inside. Regardless of the grid pattern, E_r regularly decreased with Max (ε), suggesting that damage phenomena occurred in the folding board structure before t2 point was reached and the buckling of panels was noticeable. The reduction of E_r was higher for the orthogonal grid in such a way that at the end of the test E_r was almost the same

regardless of the grid pattern. As a conclusion, the printed grid could not limit the occurrence of damage in the folding board structure but only improve the performance in the elastic domain, especially the critical buckling load of the panels. This was to be expected regarding the contribution of grid printing to the bending stiffness of the folding board (see Table 1). The box printed with the sinusoidal pattern had E_r in the same range than the reference box regardless of the Max (ε). It suggested that the sinusoidal grid affected the mechanical performance of the box early on, especially by inducing a different buckling shape (Fig. 2d).

3.2. Mechanical performance in humid atmosphere

Figure 4 depicts the unloading-loading curves of the reference box and of some printed boxes that were tested in humid atmosphere. Same typical stages were observed than under standard conditions. Same panel buckling phenomena occurred. However, the level of the plateau was at least two times lower (see Figure 5). It was expected since moisture is known to affect bonding in cellulosic fibre networks formed by papermaking as well as the mechanical behaviour of fibres themselves. The contribution of the grid to the mechanical performance was greater than in standard conditions, as expected since PLA is less sensitive to water than cellulosic fibres. The highest Max$\sum$ was also recorded for the orthogonal grid. It was also higher when the box was printed inside. The gain reached 60% in this case (see Table 2). It reached 38% for the sinusoidal grid. The evolution of E_r with Max (ε) followed the same trend than under standard conditions. As under standard conditions, the printed grid could not limit the occurrence of damage in the folding board structure, but delay the propagation of creases initiated at the corners and thus the box collapse.

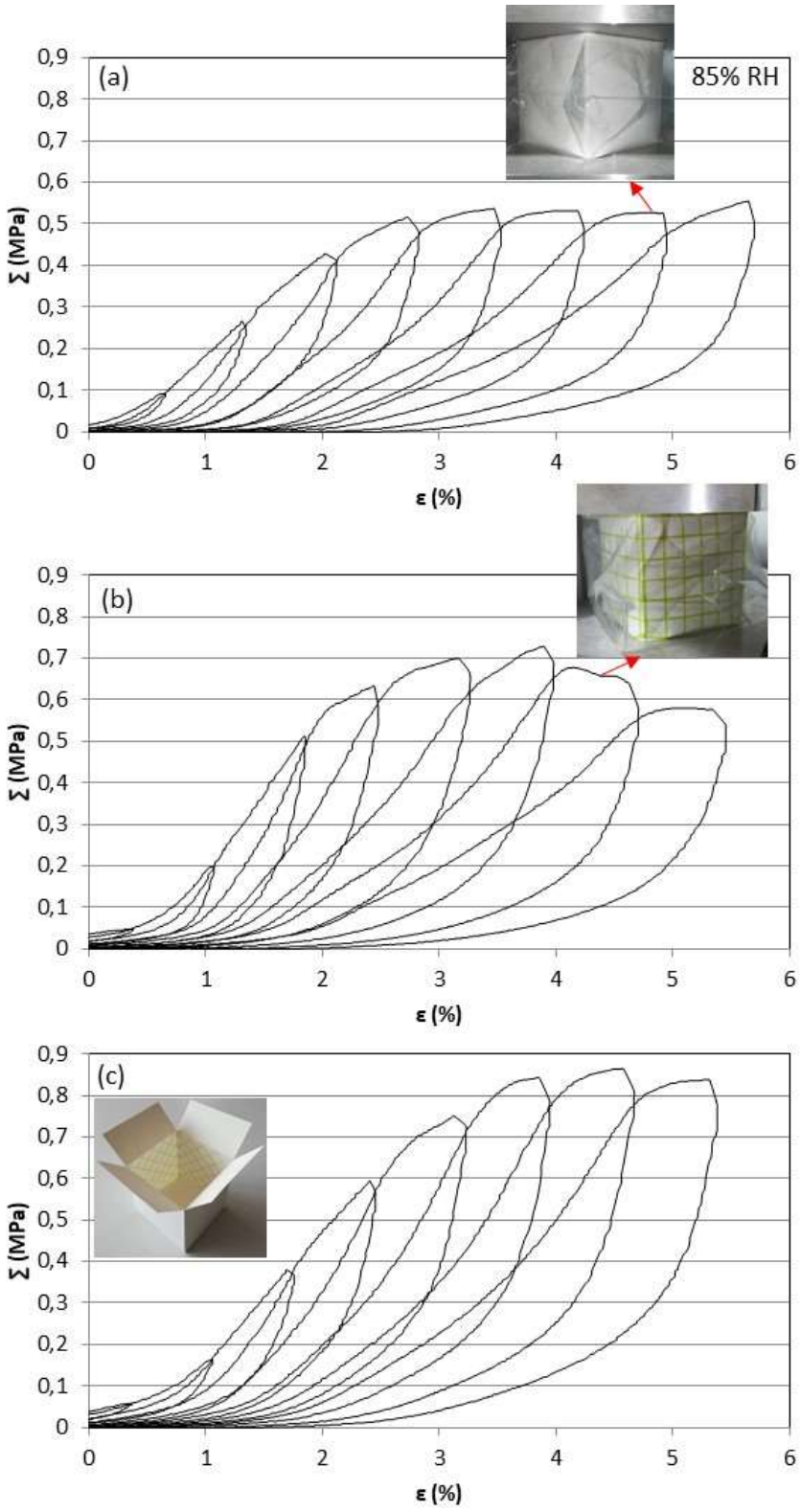

Figure 4. Loading and unloading evolution curves of (a) the reference (unprinted) box and of the boxes printed (b) on the outer side of the panels with the orthogonal grid and (c) on the inner side of the panels with the orthogonal grid orientated at 45°, with pictures of the boxes at different stages of compression.

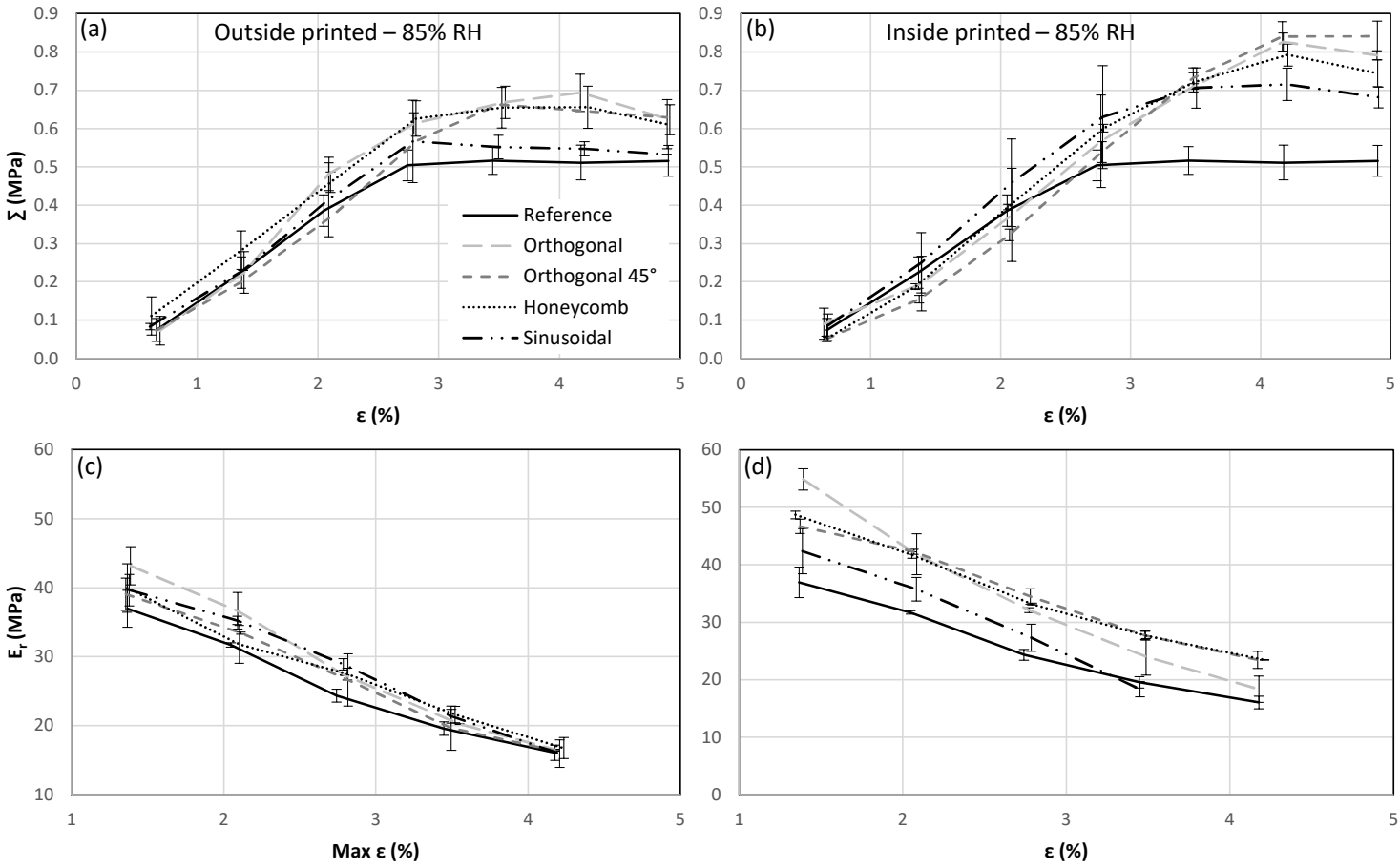

Figure 5. Same curves as in Figure 3 when boxes were tested at 85% relative humidity.

4. DISCUSSION

Results showed that printing a PLA-based grid on box panels was relevant to improve the box performance in compression, especially when it was exposed to humid conditions. By only adding 7% in weight of PLA to the whole packaging, the recorded maximum stress was improved by 29% under standard conditions and 60% in humid conditions, when the inner surface of box panels was printed with an orthogonal-type grid (Table 2). The basis weight of the folding board used to form the box could be substantially reduced. Indeed, the performance in humid conditions was at least similar to the performance of a box made with the same type of folding board with a higher basis weight of 300 g/m² (see Table 2). This suggested that the

box weight could be reduced by 30%. Knowing that PLA is only twice as expensive than paper pulp (1.5 k€/t *vs* 0.8 k€/t), the PLA grid printing approach would be relevant even considering the additive cost of FDM printing. Besides, printing on the inner side of the panels would not interfere with the conventional printing of the outside of the box or with the converting operations.

Results suggested that the grid mainly improved the elastic behaviour of panels. This could delay the buckling of panels and thus the initiation and the propagation of creases that occurred in the post-buckling regime and that were responsible of the box collapse. However, the mechanical performance as well as the buckling shape that the panels took highly depended on the grid pattern. Indeed, a pattern that forms a structure with an auxetic behaviour (*i.e.* sinusoidal-type) could affect the buckling shape, the critical buckling load since they are interdependent (Reddy, 1997), thus the stress field in the panels and finally the box collapse. This suggested that the box compression behaviour could be interestingly monitored by tuning the pattern of the printed grid. Nevertheless, this relationship should be further investigated, for instance by assessing the kinematic fields at the box panel surfaces during the compression test.

CONCLUSION

Printing a PLA grid by FDM on panels of folding board boxes was found to be relevant to improve their vertical compression behaviour. The best performances were obtained (i) with the orthogonal grid, when it was aligned with the folding board directions (MD and CD) or when it was orientated at 45° and when the grid was printed inside the box (>20%). The gain reached 60% when the box was tested under humid conditions. A comparison with a higher basis weight folding board suggested that 30% of raw materials could be saved. The printed grid could mainly improve the elastic properties of panels, delaying the buckling of panels and the phenomena responsible for box collapse. Furthermore, the grid pattern could affect the

buckling shape of the panels. This should be further investigated in view of being able to monitor the box compression behaviour by tuning the grid pattern.

DECLARATIONS

Conflicts of interest/Competing interests

Not applicable

Availability of data and material

The authors confirm that the data supporting the findings of this study are available within the article.

Code availability

Not applicable

REFERENCES

Fellers, C., & Carlsson, L. A. (2002). Bending stiffness with special reference to paperboard. *Handbook of Physical Testing of Paper*, *1*, 233.

Kabir, S., Kim, H., & Lee, S. (2020). Characterization of 3D printed auxetic sinusoidal patterns/nylon composite fabrics. *Fibers and Polymers*, *21*(6), 1372-1381.

Laszczyk, L. (2011). Homogenization and topological optimization of architectured panels. *PhD thesis, Grenoble University.*

Ren, X., Das, R., Tran, P., Ngo, T. D., & Xie, Y. M. (2018). Auxetic metamaterials and structures: a review. *Smart materials and structures*, *27*(2), 023001.

Shigemune, H., Maeda, S., Hara, Y., & Hashimoto, S. (2014, September). Design of paper mechatronics: Towards a fully printed robot. In *2014 IEEE/RSJ International Conference on Intelligent Robots and Systems* (pp. 536-541). IEEE.

Smardzewski, J. (2013). Elastic properties of cellular wood panels with hexagonal and auxetic cores. *Holzforschung*, *67*(1), 87-92.

Viguié, J. & Dumont, P. J. J. (2013). Analytical post-buckling model of corrugated board panels using digital image correlation measurements. *Composite Structures*, *101*, 243-254.

Wang, D., Abdalla, M. M., & Zhang, W. (2017). Buckling optimization design of curved stiffeners for grid-stiffened composite structures. *Composite Structures*, *159*, 656-666.

Kabir, S., Kim, H., & Lee, S. (2020). Characterization of 3D printed auxetic sinusoidal patterns/nylon composite fabrics. *Fibers and Polymers*, *21*(6), 1372-1381.

Frank, B. (2014). Corrugated box compression—a literature survey. *Packaging Technology and science*, *27*(2), 105-128.

Urbanik, T. J., & Frank, B. (2006). Box compression analysis of world-wide data spanning 46 years. *Wood and fiber science*, *38*(3), 399-416.

Li, Y., Stapleton, S. E., Reese, S., & Simon, J. W. (2016). Anisotropic elastic-plastic deformation of paper: In-plane model. *International Journal of Solids and Structures*, *100*, 286-296.

Viguié, J., Dumont, P. J., Desloges, I., & Mauret, É. (2010). Some experimental aspects of the compression behaviour of boxes made up of G-flute corrugated boards. *Packaging Technology and Science: An International Journal*, *23*(2), 69-89.

Tyagi, P., Salem, K. S., Hubbe, M. A., & Pal, L. (2021). Advances in barrier coatings and film technologies for achieving sustainable packaging of food products–a review. *Trends in Food Science & Technology*.

Valerga, A. P., Batista, M., Salguero, J., & Girot, F. (2018). Influence of PLA filament conditions on characteristics of FDM parts. *Materials*, *11*(8), 1322.

Hubbe, M. A. (2014). Prospects for maintaining strength of paper and paperboard products while using less forest resources: A review. *BioResources*, *9*(1), 1634-1763.

Lamb, M. J., & Rouillard, V. (2017). Static and dynamic strength of paperboard containers subjected to variations in climatic conditions. *Packaging Technology and Science*, *30*(3), 103-114.

Reddy, J. N., & Reddy, J. N. (1997). *Mechanics of laminated composite plates and shells: theory and analysis*. CRC press.